

## Method of Measurements of Relative Permittivity and Dielectric Loss Tangent of Micropowders in a Wide Frequency Range

A.O. Dumik<sup>1</sup>, A.A. Kalenyuk<sup>1,2</sup>, V.O. Moskaliuk<sup>1,2</sup>, A.P. Shapovalov<sup>1,2</sup>, S.I. Futimsky<sup>1</sup>, O.G. Turutanov<sup>3</sup>,  
V.Yu. Lyakhno<sup>3</sup>

<sup>1</sup> G.V. Kurdyumov Institute for Metal Physics, NAS of Ukraine, 6, Academician Vernadsky Blvd.,  
03142 Kyiv, Ukraine

<sup>2</sup> Kyiv Academic University, 03142 Kyiv, Ukraine

<sup>3</sup> Verkin Institute for Low Temperature Physics and Engineering, NAS of Ukraine, 7, Nauky Ave.,  
61103 Kharkiv, Ukraine

(Received 08 February 2022; revised manuscript received 19 April 2022; published online 29 April 2022)

Dielectric and magnetic powders find their use in a wide spectrum of scientific and technical tasks. For example, micropowders are used as a base of microwave absorbing coverage for the reflection reduction of the electromagnetic waves in the anti-radar systems. In the modern quantum computing and ultra-low noise detectors, they are used as a filling of the coaxial thermal blocking filters. Such filters are extremely necessary to ensure the noise shielding of deeply cooled devices from the measurement equipment under room temperature. For correct calculations of devices based on micropowders, it is essential to obtain their dielectric and magnetic properties. For this reason, parallel plates and induction techniques are used in the low-frequency range, and waveguide methods are used in the HF and SHF ranges. An experimental method for determining the dielectric and magnetic properties of micropowders that covers the meter to centimeter range is proposed. The main idea is to measure frequency dependences of losses and phase changes of the signal transmitted through a coaxial line segment with powder filling. Using the stated technique, we perform the measurements of graphene oxide, graphite and carbonyl iron micropowders, and the values of relative permittivity/permeability and loss tangent in the range 300 kHz – 26.5 GHz are obtained. The structural analysis of the shape and dimensions of micropowders grains is given. Determination of a reliable frequency range for measuring the dielectric/magnetic parameters of investigated micropowders is obtained, and the sensitivity of the offered technique is estimated.

**Keywords:** Coaxial line, Micropowders, Relative permittivity, Dielectric loss tangent, Phase change, Graphene oxide.

DOI: [10.21272/jnep.14\(2\).02006](https://doi.org/10.21272/jnep.14(2).02006)

PACS numbers: 41.20.Jb, 84.40. – x, 84.30.Vn,  
61.43.Gt

### 1. INTRODUCTION

Magnetic and dielectric micropowders are frequently used as electromagnetic SHF waves absorbers. For example, such structures can act as a base of paint, which is being used for stealth technology planes coverage. Powders are also being used in SHF filters, which are extremely important for shielding quantum systems and devices. Therefore, rapid determination of dielectric properties of powders in RF range is needed.

Several methodologies for measuring relative permittivity and dielectric loss tangent have been known for a long time. Most of them can be performed with different types of dielectrics: solids, liquids [1-3], thin films [4], powders, etc. The most frequently used are the parallel plate method, waveguide method, resonant techniques and bridge method. Which method should be used depends mainly on the operating frequency range, desired precision, and complexity of implementation. Let us look through the main methodologies.

In a low-frequency range (less than 100 MHz), the parallel plate method is frequently used [3]. The main idea of this technique is that investigated dielectric sample (either solid or liquid) is placed between capacitor plates thus changing its characteristics. After that, taking into account the known formulas for capacitance one can measure sample relative permittivity  $\epsilon$ . For dielectric loss tangent measurements, the following formula is being used:

$$\operatorname{tg}\delta = \omega(R + \rho)C,$$

where  $R$  is the resistance of the sample,  $\rho$  is the resistance of the parallel-connected electrode. The biggest advantage of this method is the simplicity of its realization, modelling, and calculations. As a disadvantage should be pointed a narrow low-frequency range. It is related to the fact, that reduction of wavelength leads to the impossibility of using lumped element scheme. In this case, the wavelength becomes comparable with capacitor sizes. Also in the HF range, the influence of parasite inductions becomes too significant.

To increase the precision of the measurements in the HF range, one can use different bridge schemes. Also, modifications of the Wheatstone bridge are being frequently used, for example, the Schering bridge [5]. There are also other methods for sensitivity improvement in HF and SHF ranges [6], but the most relevant ones are the use of resonant circuits.

Performing measurements of microwave properties often requires complicated and high-precision equipment [7, 8]. Resonant techniques can be conditionally divided into 2 groups: those using oscillating circuits (up to 100 MHz) and volume (cavity) resonators (> 100 MHz) [1]. The main idea of such methods is to observe resonant curves and various frequency-dependent characteristics of the system where an investigated sample is implemented. The impossibility of using oscillating circuits at frequencies higher than

100 MHz is due to strong influence of parasitic parameters, couplings, and radiation of energy into open space, thus increasing the error of measurement. Cavity resonator method provides the opportunity of performing measurements even in the SHF range [9]. Noting the changes of resonant frequency and quality factor with implemented sample, one can get the real and imaginary parts of the complex permittivity:

$$\begin{aligned}\varepsilon &= \varepsilon_1 + i * \varepsilon_2 \Delta f = -a * (\varepsilon_1 - 1), \\ \Delta \left( \frac{1}{Q} \right) &= 2a\varepsilon_2.\end{aligned}$$

This method grants high precision and the possibility to measure liquid dielectrics [10]. Disadvantages are performing measurements on a discrete frequency spectrum (resonant frequencies) and the impossibility to use with powders.

Also, in HF and SHF (> 1 GHz and < 60 GHz) ranges waveguides techniques are frequently used [4]. Most of these methods are based on the measurement of impedance of the systems, in which a sample is placed. Measuring the length of stationary waves inside the waveguide, one can obtain relative permittivity as:  $\varepsilon = \left( \frac{\lambda}{\lambda_0} \right)^2 (1 - k^2)$ , here  $k$  is the absorption coefficient. One should be very cautious while measuring solid and powder structures with the waveguide method, as the appearance of even a minimal gap between the sample and the sidewall dramatically increases the error. On the one hand, the use of circular and rectangular waveguides at frequencies above 50 GHz becomes inexpedient due to very small sample sizes. On the other hand, it is also inadvisable below 10 GHz due to large sizes of required waveguide, thus leading to the necessity of large sample sizes.

In our paper, we develop a non-resonant method for determining the dielectric properties of micropowders in the 300 kHz – 26.5 GHz range. This method is based on vector measurements of microwave characteristics of a coaxial transmission line filled with the powder. This method fills the frequency “gap” between measurements performed on circuits with lumped and distributed elements.

## 2. EXPERIMENTAL DETAILS

### 2.1 Sample Fabrication

The copper coaxial line segments to be filled with the powder were produced. They consist of a copper tube with an inner diameter of 4.83 mm and a central conductor with 0.12 mm diameter. The inner side of the tube has polished surface. The SMA connectors were placed on the edges (Fig. 1a).

Such systems are frequently used as powder filters

in projecting electromagnetic shielding schemes, with an idea to protect fragile quantum systems, for example, qubits [11]. Investigated frequency range becomes especially important due to the necessity of broadband filtration of Planck radiation during the transition to cryogenic temperatures (less than 1 K) from room temperatures (300 K) [12, 13]. Furthermore, if AC is used, eddy current losses will appear in the conductor, which are not essential at room temperature, but at low temperatures can cause conductive material heating due to its low heat capacity thus increasing its resistivity. In ferromagnetic materials, there is also additional heating related to hysteresis losses when AC is passing through.

The three types of powders frequently used as an absorbing material in powder filters were investigated (Fig. 2). These types are:

- 1) conductive graphite powder GSM-1,
- 2) ferromagnetic powder carbonyl iron P-10 (radio-technical carbonyl iron),
- 3) graphene oxide (laboratory-fabricated powder).

The raw material was graphite powder from paragraph 1. The procedure of producing graphene oxide is particularly described in [14]. The in-detail description of the possible implementation of graphene and its variations as electromagnetic shielding materials is given by overview [15].

### 2.2 Performing Measurements

All frequency-dependent measurements were performed with Vector Network Analyzer (VNA) Keysight P9375A (Fig. 1b) and two high-quality SHF-cables with a low value of the standing wave ratio. The cables were connected to pins 1 and 2 of VNA (Input and Output, correspondingly). Thus, a two-port network system for measurements was realized. Unlike a single-port network, two-port systems have shown their high efficiency in determination even small losses (0.1 dB) in superconducting non-linear microwave transmission lines [16, 17].

The calibration of VNA with SHF-cables connected was made prior to the measurements in the whole frequency range (300 kHz – 26.5 GHz). For this purpose, the automatic calibrator N7555A (Fig. 1c) was used. After the calibration, the coaxial line segment-under-test was placed between the cables. Performed calibration allowed us to avoid the influence of cables and other parasite resonances on the measurements.

As a result of signal transition through the segment of the coaxial line its power dissipates and its phase changes. The use of a VNA allowed us to obtain the required frequency characteristics of active and reactive losses.



Fig. 1 – a) Segment of a coaxial line, b) vector network analyzer, c) automatic calibration tool

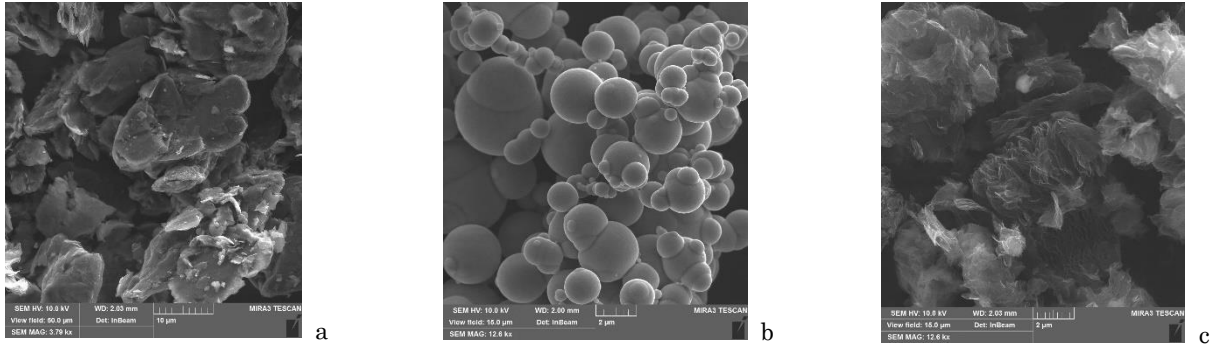


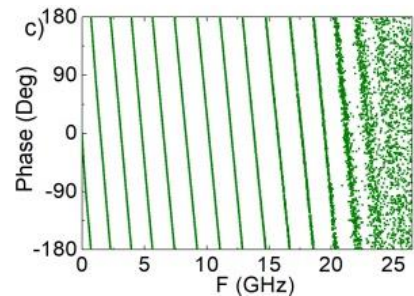
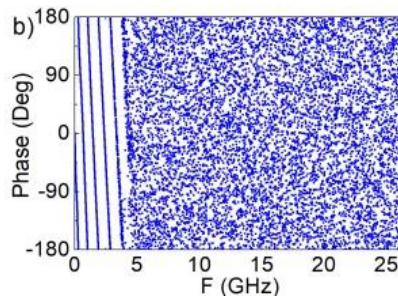
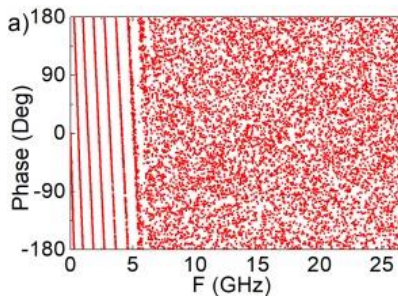
Fig. 1 – SEM images of the powder structure: a) graphite, b) carbonyl iron, c) graphene oxide

2.3 Measurement Results

The dependence of the signal phase on frequency is presented in Fig. 3a-c. The phase change periodicity for all samples is observed. The above calibration allowed us to avoid undesirable phase change related to SHF-cables. Thus, these characteristics describe only the investigated material. Fig. 3d-f shows IL (Insertion Losses, S12) versus signal frequency. IL is defined as the ratio of the powers of the incident and transmitted waves (this parameter corresponds to active losses of the line). In the whole investigated range, until the noise floor, the near-linear characteristic is observed. The filling powder determines the slope of the line. Micro powders greatly influence the line losses, as losses in the similar empty line do not exceed a few dB in the whole frequency range. Also, the methods exist for determining the dielectric properties in a coaxial line by measuring Return Losses (RL, S11) [18].

Strict periodicity of the phase as a function of frequency, and almost linear dependence of IL on frequency evidence for a common mechanism of losses appearance in the whole frequency range.

3. DISCUSSION



3.1 Refractive Index

The wavelength of the electromagnetic wave in free space  $\lambda_0$  can be determined as:

$$\lambda_0 = c/f, \tag{1}$$

where  $c$  is the speed of light in vacuum,  $f$  is the wave frequency. When a signal propagates through a coaxial line, its wavelength  $\lambda$  shortens:

$$\lambda_0/\lambda = \sqrt{\mu\epsilon}, \tag{2}$$

where  $\mu$  and  $\epsilon$  are the relative permeability and relative permittivity, respectively. Moreover, due to the fact that the coaxial line has a nonzero length, the phase changes can be noticed between the edges of the line. A phase change of  $2\pi$  appears when the signal wavelength becomes commensurate with the coaxial line segment length:

$$l = n \cdot \lambda, \tag{3}$$

where  $n$  is an integer. The frequency difference between such phase changes will correspond to frequency:

$$F = F_{n+1} - F_n. \tag{4}$$

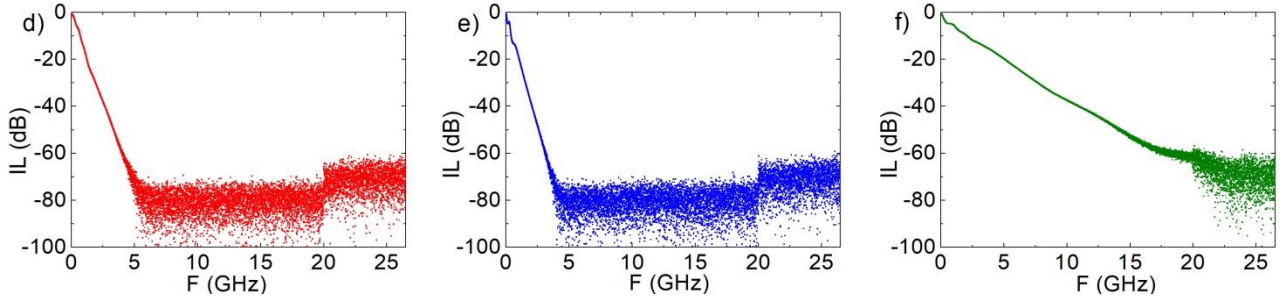


**Fig. 3** – Phase and IL of the signal transmitted through the coaxial line vs. frequency for filling powders: a) and d) graphite; b) and e) carbonyl iron; c) and f) graphene oxide

In Fig. 4a, one can see linear dependences of frequency  $F_n$  on the number of phase change points obtained from Fig. 3. Every value of  $F_n$  corresponds to a phase change of 180 deg. The slope of these linear characteristics is equal to the mean value of  $F$  obtained from (4). Substituting obtained values into (1), the wavelength in free space  $\lambda_0$  was found. In the experiment, the real wavelength of the wave  $\lambda$  corresponds to the coaxial line size (3,  $n = 1$ ). Therefore, by substituting the wavelength values  $\lambda_0$  and  $\lambda$  into (2), the magnitude of the refractive index  $\sqrt{\mu\epsilon}$  was obtained for all powders. The calculated values are given in Table 1.

### 3.2 Dielectric Loss Tangent

Dielectric loss tangent  $\text{tg}\delta$  determines the active losses in the material. For a coaxial line segment, active losses can also be determined through the attenuation constant  $\alpha$  which is proportional to the line IL [18]:

$$\alpha = 8.686 \cdot \text{IL} \cdot l. \quad (5)$$

On the other hand, the attenuation constant is composed of the conductor losses constant  $\alpha_c$  and the dielectric losses constant  $\alpha_d$ :

$$\alpha = \alpha_c + \alpha_d. \quad (6)$$

In the case of a coaxial transition line, the losses in the conductor can be calculated as [19]:

$$\alpha_c = \frac{R_s}{2\sqrt{\mu_0/\epsilon_0\epsilon_r} \ln(b/a)} \left( \frac{1}{a} + \frac{1}{b} \right), \quad (7)$$

where  $R_s$  is the surface resistance of the central conductor material:

$$R_s = \frac{\rho}{\Delta}, \quad (8)$$

where  $\Delta$  is the skin layer depth:

$$\Delta = \sqrt{\frac{\rho}{\pi\mu_0\mu f}}.$$

The dielectric loss constant can be calculated as:

$$\alpha_d = \frac{2\pi f}{2} \sqrt{\mu_0\epsilon_0\epsilon} \text{tg}\delta. \quad (9)$$

Fig. 4b shows the dependences of the attenuation constant  $\alpha$  on the frequency calculated by (5) for different fillings of the coaxial line and the theoretically determined attenuation constant (7), (8) for an empty

line (air). It follows from (7) and (8) that conductor losses are proportional to the square root of the frequency,  $\alpha_c \sim \sqrt{F}$ , and, from (9), that dielectric losses are proportional to the signal frequency,  $\alpha_d \sim F$ . Therefore, by obtaining the linear dependences  $\alpha \sim F$  in the experiment for each sample, we can conclude that dielectric or magnetic losses are dominant in the coaxial line.

By obtaining the slope of the linear characteristics of the attenuation constant (Fig. 4b) and using (9), the dielectric loss tangent  $\text{tg}\delta$  was calculated for each powder. The results are presented in Table 1.

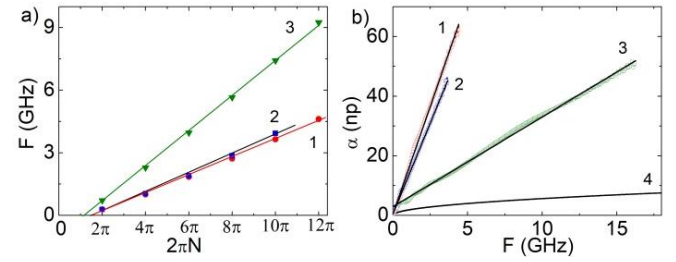


**Fig. 4** – a) Frequencies corresponding to periodical  $2\pi$ -fold phase changes vs. phase change and b) attenuation constant  $\alpha$  vs. frequency for the coaxial line filled with: 1 – graphite, 2 – carbonyl iron, 3 – graphene oxide, 4 – air (theoretical calculation)

### 3.3 Critical Frequency

The above method of dielectric loss tangent and refractive index determination has its own critical frequencies. The first (upper) one is related to change of the type of electromagnetic wave in the coaxial line:

$$f_{cup} = \frac{c}{\lambda_c} = \frac{2 \cdot c}{(D+d)\pi\sqrt{\epsilon}}. \quad (10)$$

When the cut-off frequency is exceeded, the longitudinal mode of TEM-wave degenerates into a single-transverse TE- or TM- modes, thus dissipating a lot during the inline propagation. The frequency at which the TE<sub>11</sub> modes firstly appear is called the maximum cut-off frequency of the coaxial line. As we see from (10), this critical frequency depends on the relative permittivity of the dielectric powder, which fills the coaxial line. Thus, we can state that our methodology is inappropriate for powders with high relative permittivity, as the cut-off frequency will be too low. With the above formula, the critical frequencies for all samples were obtained as follows:  $f_{cup}(\text{Fe}) = 8.543$  GHz,  $f_{cup}(\text{graphite}) = 12.337$  GHz,  $f_{cup}(\text{graphene}) = 23.613$  GHz. Since the transmission characteristics reach the noise

floor at lower frequencies (Fig. 3d-f), it is impossible to determine the cut-off frequencies from experiment.

**Table 1** – Obtained values of the refractive index  $n^2 = \epsilon\mu$  and dielectric loss tangent for all samples

Filling	Line length, cm	$\epsilon\mu$	$\text{tg}\delta$
Graphite	7.3	9.459	0.49
Carbonyl iron	7.4	19.724	0.65
Graphene oxide	10.4	2.582	0.24

The lower critical frequency estimation is determined by the sensitivity of VNA and losses in the powders. Let us set the criterion  $IL_{\min} = 1$  dB for the reliable determination of losses in the coaxial line. Then according to (5) and (9)

$$f_{\text{down}} = \frac{8.686 \cdot IL \cdot l}{\pi \sqrt{\mu_0 \cdot \epsilon_0 \epsilon \cdot \text{tg}\delta}} \quad (11)$$

The critical frequencies calculated from (11) are:  
 $f_{\text{down}}(\text{Fe}) = 40.256$  MHz,  $f_{\text{down}}(\text{graphite}) = 41.002$  MHz,  
 $f_{\text{down}}(\text{graphene}) = 228.18$  MHz.

## REFERENCES

1. A.A. Brandt, *Issledovaniya dielektrikov na sverkhvysokikh chastotakh* (Moskva: gos. izd. fiz.-mat. literatury: 1963) [In Russian].
2. S.O. Nelson, *Trans. ASABE* **42** No 2, 523 (1999).
3. V.M. Radivojevic, S. Rupcic, M.Srnovic, G. Bencic, *IJECE* **9**, 1 (2018).
4. B.-K. Chung, *PIER* **75**, 239 (2007).
5. S.C. Bera, D.N. Kole, *Sens. Transducers* **96** No 9, 104 (2008).
6. J.L. Oncley, *Am. Chem. Soc.* **60**, 1115 (1938).
7. A.F. Harvey, *Microwave Engineering* (Moskva: Sovetskoe Radio: 1965).
8. V. Bovtun, V. Pashkov, M. Kempa, *J. Appl. Phys.* **109**, 024106 (2011).
9. Y.V. Didenko, V.I. Molchanov, V.M. Pashkov, D.D. Tatarchuk, D.A. Shmyhin, *Electronics and Communications* **19** No 6, 14 (2014).
10. H. Hamzah, J. Lees, *Sensor. Actuat. A* **276**, 1 (2018).
11. V.I. Shnyrkov, A.M. Korolev, O.G. Turutanov, V.M. Shulga, V.Yu. Lyakhno, V.V. Serebrovsky, *Low Temp. Phys.* **41**, 867 (2015).
12. V.I. Shnyrkov, Wu Yangcao, A.A. Soroka, O.G. Turutanov, V.Yu. Lyakhno, *Low Temp. Phys.* **44**, 213 (2018).
13. A.M. Korolev, V.M. Shulga, O.G. Turutanov, V.I. Shnyrkov, *Solid State Electron.* **121**, 20 (2016).
14. A.V. Dolbin, N.A. Vinnikov, V.B. Esel'son, V.G. Gavrilko, R.M. Basnukaeva, *Low Temp. Phys.* **46** No 3, 293 (2020).
15. Z. Jia, M. Zhang, B. Liu, F. Wang, G. Wei, Z. Su, *ACS Appl. Nano Mater.* **3**, 6140 (2020).
16. A.A. Kalenyk, *Low Temp. Phys.* **35**, 105 (2009).
17. A.A. Kalenyuk, A.I. Rebikov, A.L. Kasatkin, V.M. Pan, *2010 International Kharkov Symposium on Physics and Engineering of Microwaves, Millimeter and Submillimeter Waves* (2010).
18. V.A. Ivanov, *X Vserosiyskaya nauchno-tehnicheskaya konfrentsiya «Elektronika i mikroelektronika SVCH»*, 595, (Sankt-Peterburg: LETI: 2021) [In Russian].
19. Devendra K. Misra, *Radiofrequency and Microwave Communication Circuits: Analysis and Design* (John Wiley & Sons, Inc.: 2001).

## Метод вимірювання діелектричної проникності та тангенса діелектричних втрат мікропорошків в широкому діапазоні частот

А.О. Думік<sup>1</sup>, О.А. Каленюк<sup>1,2</sup>, В.О. Москалюк<sup>1,2</sup>, А.П. Шаповалов<sup>1,2</sup>, С.І. Футимський<sup>1</sup>, О.Г. Турутанов<sup>3</sup>, В.Ю. Ляхно<sup>3</sup>

<sup>1</sup> Інститут металофізики імені Г.В. Курдюмова НАН України, бульвар Акад. Вернадського, 36, 03142 Київ, Україна

<sup>2</sup> Київський академічний університет, бульвар Акад. Вернадського, 36, 03142 Київ, Україна

<sup>3</sup> Фізико-технічний інститут низьких температур імені Б.І. Веркіна НАН України, проспект Науки, 47, 61103 Харків, Україна

Діелектричні та магнітні мікропорошки знайшли своє призначення у широкому спектрі науково-технічних задач. Наприклад, мікропорошки застосовують як основу поглинаючих мікрохвильових покриттів для зменшення відбиття хвиль в антирадарних системах. У надсучасних квантових обчислювальних схемах і детекторах з наднизьким рівнем шуму, мікропорошки використовуються як наповнювачі коаксіальних термоблокуючих фільтрів. Такі фільтри вкрай необхідні для забезпечення шумової ізоляції глибоко охолоджених пристроїв від вимірювальної апаратури, яка знаходиться при кімнатній температурі. Для розрахунків пристроїв на основі мікропорошків необхідно отримати їх діе-

лектричні та магнітні характеристики. Для цього на низьких частотах використовують конденсаторні або індуктивні методи, а на мікрохвильових частотах – хвилеводні методи. В роботі запропоновано метод визначення діелектричних та магнітних характеристик мікропорошків для покриття проміжного діапазону метрових та сантиметрових довжин хвиль. Метод базується на вимірюванні частотних залежностей втрат та зміни фази сигналу, що проходить скрізь відрізок коаксіальної лінії передачі з мікропорошковим наповненням. З використанням запропонованого метода проведені дослідження мікропорошків з оксиду графену, графіту та карбонільного заліза та знайдені значення їх діелектричних/магнітних проникностей та тангенсів втрат в діапазоні частот 300 кГц – 26.5 ГГц. Приведено структурний аналіз форми та розмірів зерен мікропорошків. Зроблені розрахунки визначення достовірного частотного діапазону для вимірювання діелектричних/магнітних параметрів досліджених мікропорошків, та проведено оцінку чутливості запропонованої методики.

**Ключові слова:** Коаксіальна лінія, Мікропорошки, Діелектрична проникність, Тангенс кута діелектричних втрат, Зміна фази, Оксид графену.